Electronic Supplementary Material (ESI) for Nanoscale.

Electronic Supplementary Information for Theory of waveguide design for plasmonic nanolasers

October 2, 2018

Guangyuan Li,*[a,b,c] Stefano Palomba,[a,d] and C. Martijn de Sterke[a,b]

[a] *Institute of Photonics and Optical Science (IPOS), School of Physics, The University of Sydney, NSW 2006, Australia*
[b] *Centre for Ultrahigh bandwidth Devices for Optical Systems (CUDOS), School of Physics, The University of Sydney, NSW 2006, Australia*
[c] *Shenzhen Institutes of Advanced Technology (SIAT), Chinese Academy of Sciences, Shenzhen 518055, China*
[d] *The University of Sydney Nano Institute, The University of Sydney, NSW 2006, Australia*

Email: G.L. (gy.li@siat.ac.cn)

S1 Modal Purcell factor and threshold gain for nanolasers

The Purcell factor of a waveguide mode can be expressed as[1]

$$F_{\mathrm{m}}(\mathbf{r_0}) = \frac{3}{4\pi}\left(\frac{\lambda}{n_0}\right)^2 \frac{\frac{1}{2}c\varepsilon_0 n_0^2|\mathbf{e}(\mathbf{r_0})|^2}{n_0\cdot\frac{1}{2}\int_\infty(\mathbf{e}\times\mathbf{h}^*)\cdot\hat{z}\mathrm{d}A}\,, \tag{S1}$$

where $\mathbf{r_0}$ is the emitter position, n_0 is the refractive index of the gain medium, λ is the wavelength, $\{\mathbf{e},\mathbf{h}\}$ are the modal fields, and $\int_\infty(\cdot)\mathrm{d}A$ is an integral over the entire cross section. Its maximum, $F_{\mathrm{m,max}}$, is

$$F_{\mathrm{m,max}} = \frac{3}{\pi}\left(\frac{\lambda}{2n_0}\right)^2 \frac{\max\{c\varepsilon_0 n_0|\mathbf{e}|^2\}_{\underline{\mathrm{D}}}}{\int_\infty(\mathbf{e}\times\mathbf{h}^*)\cdot\hat{z}\mathrm{d}A}\,, \tag{S2}$$

which can be rewritten as Eq. (1) in the main text with the diffraction-limited area $A_0 \equiv (\lambda/(2n_0))^2$ and the effective area A_{eff} defined by Eq. (2) in the main text. Here $\max\{\cdot\}_{\underline{\mathrm{D}}}$ indicates the maximum over the gain medium ("$\underline{\mathrm{D}}$").

A conventional definition of effective area is the ratio of the total mode energy and the peak energy density[2],

$$A_{\mathrm{eff,C}} \equiv \frac{\int_\infty W\mathrm{d}A}{\max\{W\}}\,, \tag{S3}$$

where $W = \frac{1}{4}\left(\varepsilon_0\frac{\partial(\omega\varepsilon_{\mathrm{r}}')}{\partial\omega}|\mathbf{e}|^2 + \mu_0|\mathbf{h}|^2\right)$ is the energy density. By assuming that $\mu_0|\mathbf{h}|^2 \approx \varepsilon_0\frac{\partial(\omega\varepsilon_{\mathrm{r}}')}{\partial\omega}|\mathbf{e}|^2$ and that the peak energy density is located in the gain medium, one can obtain[3]

$$F_{\mathrm{m,max}} \approx \frac{3}{\pi}\frac{n_{\mathrm{e}}}{n_0}\frac{A_0}{A_{\mathrm{eff,C}}}\,. \tag{S4}$$

Here $n_{\mathrm{e}} = c/v_{\mathrm{e}}$ is the energy velocity index, and $v_{\mathrm{e}} = \frac{1}{2}\int_\infty(\mathbf{e}\times\mathbf{h}^*)\cdot\hat{z}\mathrm{d}A\Big/\int_\infty W\mathrm{d}A$ is the energy velocity.

For conventional, all-dielectric lasers, $\max\{\cdot\}_{\underline{\mathrm{D}}}$ is equivalent to $\max\{\cdot\}$, the maximum value over the entire cross section, because the peak electric energy is located in the gain medium. This is not so for plasmonic lasers for which the peak electric energy can be located elsewhere, necessitating an explicit reference to the maximum in the gain medium. Furthermore, $A_{\mathrm{eff}} = n_0/n_{\mathrm{e}}\cdot A_{\mathrm{eff,C}}$ by comparing Eqs. (S2) and (S4). Therefore, the effective area defined by Eq. (2) in the main text is more complete than the conventional definition by Eq. (S3).

For plasmonic nanolasers, the dominating loss is the waveguide modal loss, which can be expressed as

$$\alpha_{\mathrm{m}} = \frac{\omega_0\varepsilon_0\int_{\mathrm{M}}\varepsilon_{\mathrm{r,M}}''|\mathbf{e}|^2\mathrm{d}A}{\int_\infty(\mathbf{e}\times\mathbf{h}^*)\cdot\hat{z}\mathrm{d}A}\,, \tag{S5}$$

hence we obtain the threshold gain,

$$g_{\mathrm{th}} \approx \alpha_{\mathrm{m}}/\Gamma_{\mathrm{G}} = k_0 n_0\frac{\int_{\mathrm{M}}\varepsilon_{\mathrm{r,M}}''|\mathbf{e}|^2\mathrm{d}A}{\int_{\underline{\mathrm{D}}} n_0^2|\mathbf{e}|^2\mathrm{d}A}\,. \tag{S6}$$

Equation (S6) can be rewritten as Eq. (4) in the main text.

S2 Figure of Merit and nonlinear effectiveness for DFWM devices

The Figure of Merit for nonlinear plasmonic waveguides is defined as[4]

$$\mathscr{F} \equiv \gamma P_{0,\mathrm{max}} L_{\mathrm{att}}\,. \tag{S7}$$

The expression of γ, the nonlinear coefficient of the plasmonic waveguide mode, was first derived by Afshar *et al.*[5] and was benchmarked by Li *et al.*[6]. $L_{\mathrm{att}} = 1/\alpha_{\mathrm{m}}$ is the attenuation length with α_{m} expressed by Eq. (S5). The maximum admissible pump power, at which the maximum nonlinear index change Δn_{max} of the material is reached, is defined as[4]

$$P_{0,\mathrm{max}} \equiv \frac{\frac{1}{2}\int_\infty(\mathbf{e}\times\mathbf{h}^*)\cdot\hat{z}\mathrm{d}A}{\max\{|\mathbf{e}|^2\}_{\underline{\mathrm{D}}}}|\mathbf{E}_{\mathrm{bulk,max}}|^2\,. \tag{S8}$$

Here $|\mathbf{E}_{\mathrm{bulk,max}}|^2$ is the maximum electric field intensity for bulk material under plane wave illumination. It can be extracted from the maximum allowed plane wave intensity through $I_{\mathrm{bulk,max}} = \frac{1}{2}c\varepsilon_0 n_0|\mathbf{E}_{\mathrm{bulk,max}}|^2$. With $I_{\mathrm{bulk,max}}$ Eq. (S8) can be rewritten as Eq. (6) in the main text. By substituting the expressions for γ, $P_{0,\mathrm{max}}$ and L_{att} into Eq. (S7), the Figure of Merit can be written as Eq. (8) in the main text.

The nonlinear effectiveness is defined as $\mathrm{EFF_{NL}} \equiv \Delta\Phi_{\mathrm{NL,m}}/\Delta\Phi_{\mathrm{NL,bulk}}$, where $\Delta\Phi_{\mathrm{NL,m}} = \gamma P_{0,\mathrm{max}}L$ is the nonlinear phase shift of the waveguide mode, and $\Delta\Phi_{\mathrm{NL,bulk}} = \Delta n_{\mathrm{max}}k_0 L$ is that of bulk material under plane wave illumination. By replacing the device L with the optimal length $L_{\mathrm{opt}} = \ln(3)L_{\mathrm{att}}$, this dimensionless parameter also applies to plasmonic waveguides. By substituting the expressions for γ, $P_{0,\mathrm{max}}$ and L_{att}, $\mathrm{EFF_{NL}}$ can be rewritten as Eq. (7) in the main text.

S3 Global comparison of 1D plasmonic waveguide configurations

For the global optimization, we first compared three-layer configurations. With the five materials of "M", "$\underline{\mathrm{D}}$", "L", "H", and "A", we find there are 10 plasmonic waveguide mode for three-layer configurations, which include the semi-infinite substrate and superstrate layers.

Figure S1 compares the characteristics of 7 three-layer plasmonic modes as a nanolaser and as a DFWM device at $\lambda = 1,550\,\mathrm{nm}$ and at $\lambda = 790\,\mathrm{nm}$, with the M$\underline{\mathrm{D}}$ (the SPP) as reference. In this figure, the characteristics of the long-range SPP (LRSPP) and the short-range SPP (SRSPP) supported by the $\underline{\mathrm{D}}$M$\underline{\mathrm{D}}$ configuration are also shown, whereas those of the AM$\underline{\mathrm{D}}$, LM$\underline{\mathrm{D}}$ and HM$\underline{\mathrm{D}}$ configurations are worse than the M$\underline{\mathrm{D}}$M and the M$\underline{\mathrm{D}}$A, and thus are not shown for clarity.

Figure S1 shows that, amongst the three-layer plasmonic waveguide modes, the M$\underline{\mathrm{D}}$M is the best in the deep- and modest-subdiffraction regions, whereas the M$\underline{\mathrm{D}}$A performs best in the near-subdiffraction region. Here the deep-, modest- and near-subdiffraction regions are defined in the main text. The M$\underline{\mathrm{D}}$A is preferred over the M$\underline{\mathrm{D}}$L. The M$\underline{\mathrm{D}}$H has the worst performance because of the small overlap between the modal electric energy and the active "$\underline{\mathrm{D}}$" medium[7]. The effective areas of the LRSPP and SRSPP modes are diffraction limited for the long operation wavelength of $\lambda = 1,550\,\mathrm{nm}$, as shown in Fig. S1(a)(b), but subdiffraction for the short wavelength of $\lambda = 790\,\mathrm{nm}$, as shown in Fig. S1(c)(d). For the ML$\underline{\mathrm{D}}$, its k_0/g_{th} and $\mathscr{F}/\Delta n_{\mathrm{max}}$ linearly scale with the increasing A_{eff}/A_0. In contrast, for the MH$\underline{\mathrm{D}}$, its k_0/g_{th} and $\mathscr{F}/\Delta n_{\mathrm{max}}$ first linearly scale with the decreasing A_{eff}/A_0, and then continue to decrease even when A_{eff}/A_0 starts to increase from the minimum value.

Through comparison of three-layer configurations, we obtained a pool of best performing configurations: the M$\underline{\mathrm{D}}$M and the M$\underline{\mathrm{D}}$A. For four-layer configurations, we globally optimized the performance k_0/g_{th} or $\mathscr{F}/\Delta n_{\mathrm{max}}$ versus A_{eff}/A_0, by varying the thicknesses of all the central layers. If the best performance is better than those of the pool, this configuration together with the optimal parameters is added to the pool, otherwise it is abandoned. The comparison of five-layer configurations is performed similarly.

S4 Similarities between plasmonic lasers and DFWM devices

Figure S2 plots the equivalent parameters between plasmonic lasers and plasmonic DFWM devices at $\lambda = 1,550\,\mathrm{nm}$: k_0/g_{th} and $\mathscr{F}/\Delta n_{\mathrm{max}}$ [Fig. S2(a)], Γ_{G} and $\mathrm{EFF}_{\mathrm{NL}}/f_\ell$ [Fig. S2(b)]. We find that $\mathscr{F}/\Delta n_{\mathrm{max}} \approx 1/2 \cdot k_0/g_{\mathrm{th}}$ and $\mathrm{EFF}_{\mathrm{NL}}/f_\ell \approx 1/2 \cdot \Gamma_{\mathrm{G}}$ for the M$\underline{\mathrm{D}}$ SPP, where the factor of 1/2 arises because $\mathscr{F}/\Delta n_{\mathrm{max}}$ and $\mathrm{EFF}_{\mathrm{NL}}/f_\ell$ include an additional U describing the field uniformity [see Eqs. (7) and (8) in the main text] and the field exponentially decays in the active "$\underline{\mathrm{D}}$" layer[7]. For other configurations with small values of $t_{\underline{\mathrm{D}}}$, $\mathscr{F}/\Delta n_{\mathrm{max}} \approx k_0/g_{\mathrm{th}}$ and $\mathrm{EFF}_{\mathrm{NL}}/f_\ell \approx \Gamma_{\mathrm{G}}$ because of the uniform fields in the active "$\underline{\mathrm{D}}$" layer. These approximations greatly simplify the design and the understanding of waveguide configurations for plasmonic lasers and DFWM devices, since in practice thin active "$\underline{\mathrm{D}}$" layers are of great interest.

Figure S2(b) also shows that the nonlinear effectiveness, just like the gain confinement factor (main text), can exceed unity for the M$\underline{\mathrm{D}}$M and MH$\underline{\mathrm{D}}$HM configurations. This is because there exist slow-light effects in these configurations with small $t_{\underline{\mathrm{D}}}$[7].

The characteristics of plasmonic lasers and DFWM devices at $\lambda = 790\,\mathrm{nm}$ are qualitatively and quantitatively similar as those at $\lambda = 1,550\,\mathrm{nm}$. Figure S3(a)(b) provides an understanding to Figs. 1(d) and 5(b) in the main text in terms of the loss and the confinement, and Fig. S3(c)(d) shows the similarities between equivalent parameters of plasmonic lasers and plasmonic DFWM devices.

Notes and references

[1] V. J. Sorger, N. Pholchai, E. Cubukcu, R. F. Oulton, P. Kolchin, C. Borschel, M. Gnauck, C. Ronning and X. Zhang, *Nano Lett.*, 2011, **11**, 4907–4911.

[2] R. F. Oulton, V. J. Sorger, D. A. Genov, D. F. P. Pile and X. Zhang, *Nat. Photon.*, 2008, **2**, 496–500.

[3] R. F. Oulton, G. Bartal, D. F. P. Pile and X. Zhang, *New J. Phys.*, 2008, **10**, 105018.

[4] G. Li, C. M. de Sterke and S. Palomba, *Laser Photon. Rev.*, 2016, **10**, 639–646.

[5] V. S. Afshar and T. M. Monro, *Opt. Express*, 2009, **17**, 2298–2318.

[6] G. Li, C. M. de Sterke and S. Palomba, *Opt. Lett.*, 2017, **42**, 1329–1332.

[7] G. Li, C. M. de Sterke and S. Palomba, *ACS Photon.*, 2018, **5**, 1034–1040.

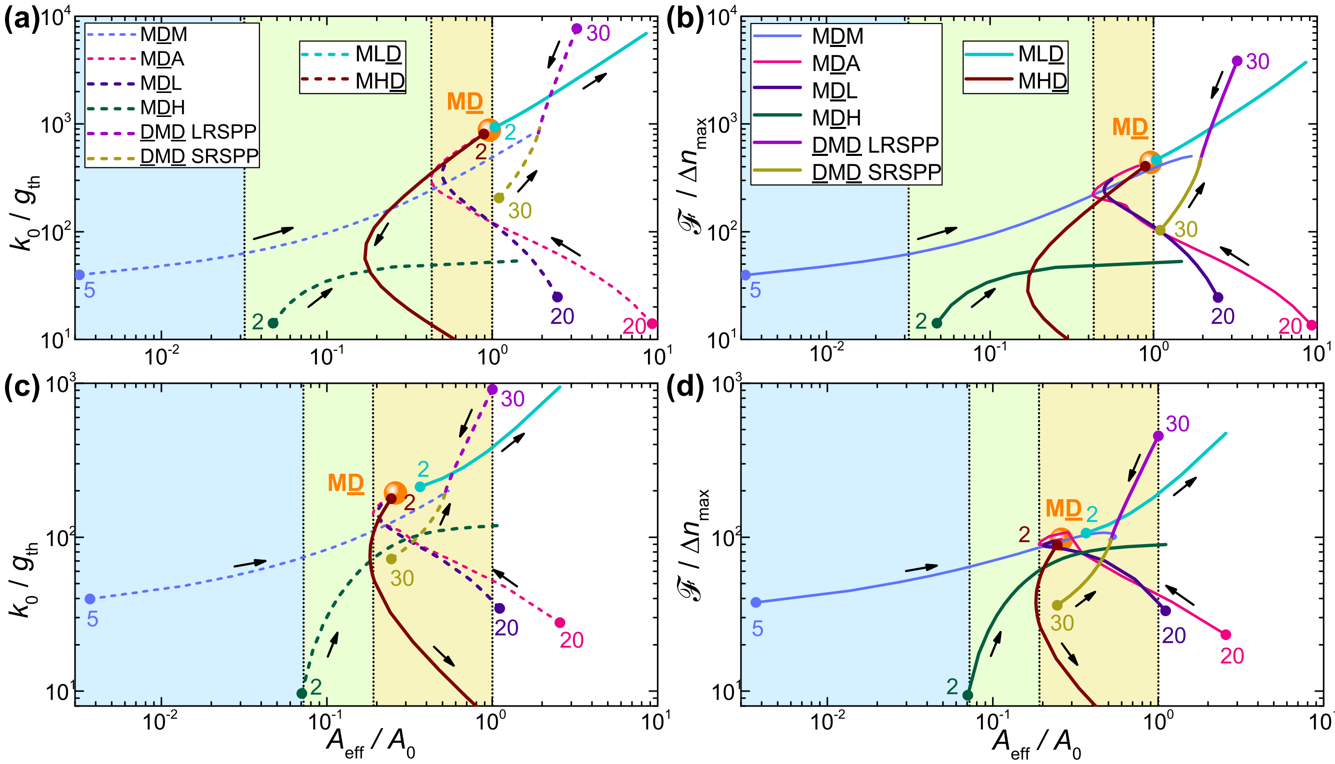

Figure S1 Characteristics of three-layer plasmonic waveguide configurations for nanolasers and DFWM devices. (a)(c) k_0/g_{th} for nanolasers, (b)(d) $\mathscr{F}/\Delta n_{\max}$ for DFWM devices versus A_{eff}/A_0, as the active "D" layer thickness t_{D} increases (indicated by arrows) from the numbers in nanometers (circles). Blue, green, yellow and white indicate deep-, moderate-, and near-subdiffraction, and diffraction-limited regions, respectively. Configurations exhibiting quenching are indicated by dashed curves. The calculations were performed with (a)(b) $\lambda = 1{,}550\,\mathrm{nm}$ and (c)(d) $\lambda = 790\,\mathrm{nm}$, and the corresponding material sets.

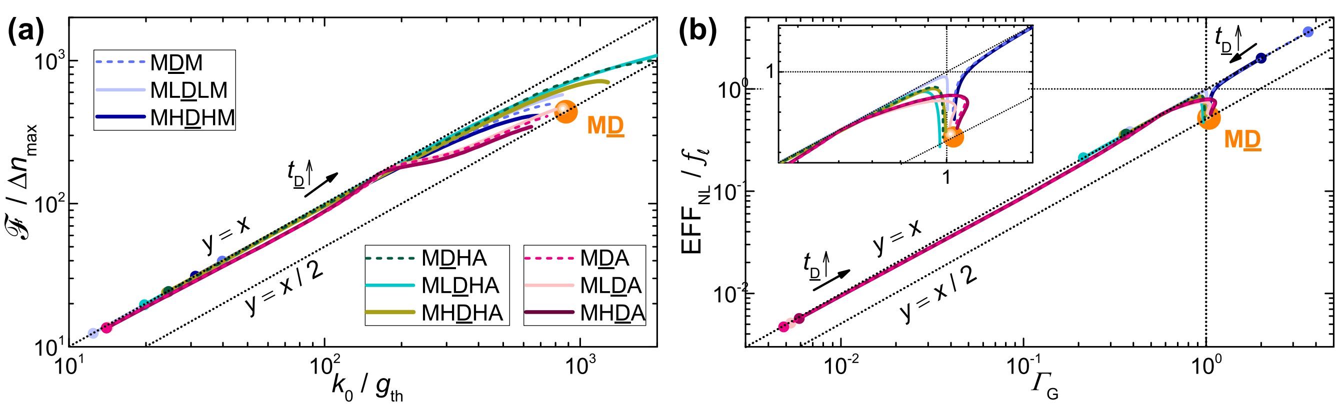

Figure S2 Comparison of optimal performing plasmonic waveguides for use as nanolasers and for use as DFWM devices at $\lambda = 1{,}550\,\mathrm{nm}$. (a) $\mathscr{F}/\Delta n_{\max}$ versus k_0/g_{th}, and (b) $\mathrm{EFF_{NL}}/f_\ell$ versus Γ_{G} with inset a zoom-in. Arrows indicate the direction of increasing of the active "D" layer thickness t_{D} from the numbers in nanometres (circles) to $1{,}300\,\mathrm{nm}$.

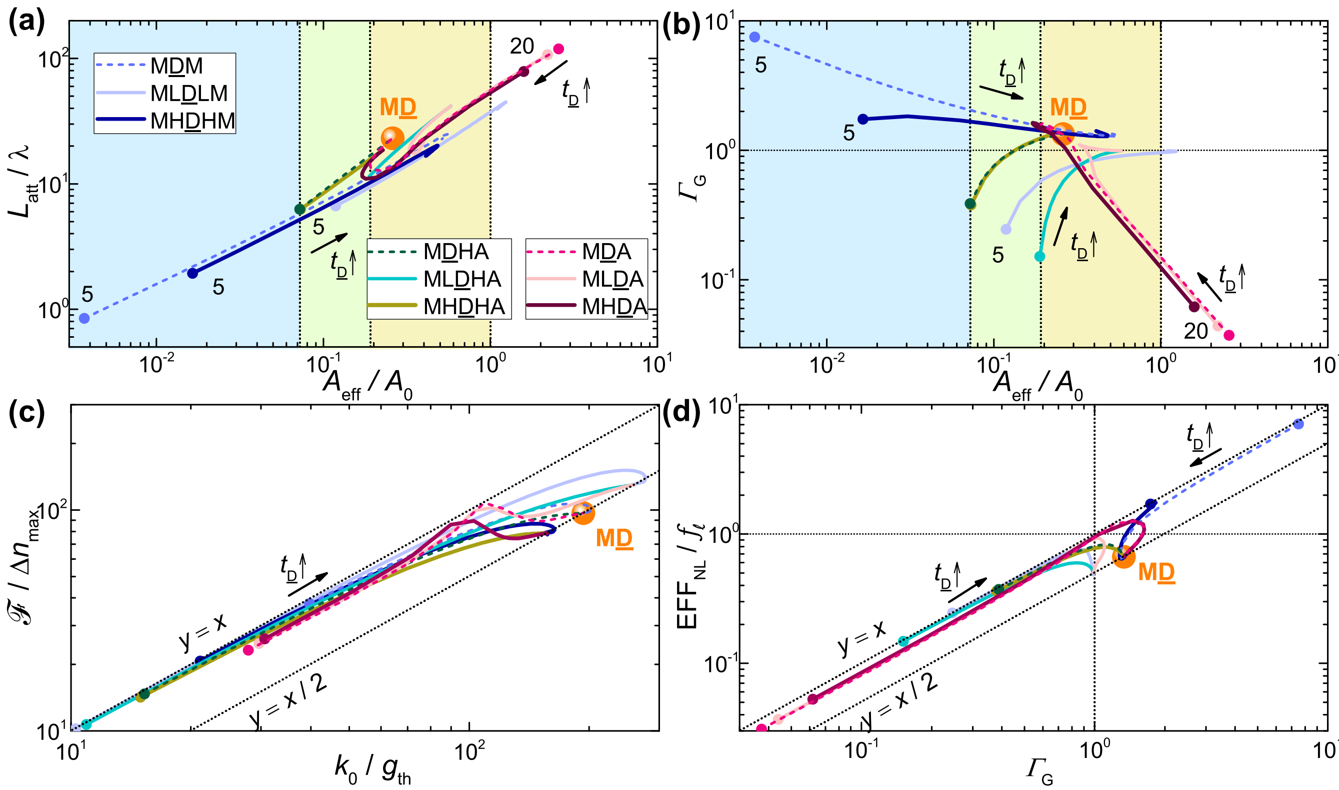

Figure S3 Characteristics of optimal performing plasmonic waveguide configurations for nanolasers and DFWM devices at $\lambda = 790$ nm. (a) L_{att}/λ and (b) Γ_G versus A_{eff}/A_0 as the active "D" layer thickness $t_{\underline{D}}$ increases from the numbers in nanometers (circles) to 1,300 nm. (c) $\mathscr{F}/\Delta n_{max}$ versus k_0/g_{th} and (d) EFF_{NL}/f_ℓ versus Γ_G.